

Metal-ion spin-on glasses: novel materials for active waveguides

Carol I.H. Ashby, Charles T. Sullivan, G. Allen Vawter, John P. Hohimer, G. Ronald Hadley,
and Daniel R. Neal

Sandia National Laboratories
Albuquerque, New Mexico 87185-0603

ABSTRACT

Monolithic integration of a rare-earth-ion-based active waveguide on the same wafer as its diode pump laser would permit compact packaging of the technology demonstrated in fiber lasers and amplifiers. This new monolithic technology would offer the potential for developing compact infrared and visible (up-conversion) lasers, amplifiers, and other photonic integrated circuit components. One approach that we are investigating for such monolithic integration uses a high concentration of one or more rare-earth ions incorporated into polysiloxane spin-on glasses that are solvent-cast onto III-V semiconductor wafers. This "fiber on a chip" technology substitutes a relatively high-ion-concentration, short-length metal-ion spin-on glass (MISOG) waveguide for the low-ion-concentration, long-length fiber. Progress to date on developing MISOG waveguide materials and technology is discussed.

1. INTRODUCTION

With the success in developing rare-earth-doped fiber lasers and amplifiers, considerable effort is now being directed toward the development of a rare-earth-doped planar waveguide technology. Such an integrated technology will allow a reduction in the size of devices, making it possible to fabricate multiple devices on a substrate; and it will allow the development of active integrated optical circuits with gain.

To date, the effort in developing a rare-earth-doped planar waveguide technology has been largely concerned with the development of stand-alone lasers or amplifiers on glass, LiNbO_3 , or silicon substrates with external laser pumping.¹ In our view, there is a need for the monolithic integration of rare-earth-doped waveguides with quantum-well pump lasers on III-V semiconductor substrates. This approach will overcome the limitations of chip-level and film-level hybrid integration techniques;² and it will allow the incorporation of essential semiconductor components including pump lasers, photodetectors, and modulators. The addition of rare-earth-doped materials to III-V semiconductor substrates will result in increased functionality compared to semiconductor photonic integrated circuits. This includes better coupling to optical fibers, access to wavelengths from the visible to the infrared, narrower lasing linewidths, Q-switching for high peak powers, femtosecond pulse generation by mode locking, and soliton pulse generation.

Several processes are currently being used to fabricate rare-earth-doped waveguide lasers and amplifiers. These fabrication processes include ion exchange, ion implantation, flame hydrolysis deposition, and electron-beam vapor deposition.¹ These processes incorporate very high temperature annealing steps that make them incompatible with quantum-well pump lasers on III-V semiconductor substrates. For this reason, we are exploring the use of a spin-on glass host material, which requires processing temperatures below 430° C, for the development of monolithic integrated rare-earth-doped photonic circuits.

Figure 1 shows two possible monolithic integrated device concepts for spin-on glass lasers and amplifiers. Figure 1(a) shows a concept for a high-power rare-earth-doped solid-state laser or amplifier formed by etching a trench several millimeters wide into a semiconductor wafer containing quantum-well graded-index separate-confinement-heterostructure (GRIN-SCH) diode array pump lasers. This trench, formed by reactive ion beam etching down through the diode laser active region, forms both the array output facet mirror and a region for the deposition of multiple spin-on glass layers that form the rare-earth-doped glass laser or amplifier. The rare-earth content of individual spin-on-glass layers are adjusted to form an optical waveguide.

In Fig. 1(b), a concept for a single-mode rare-earth doped waveguide amplifier is shown with evanescent laser pumping. The channel for deposition of the layered spin-on glass waveguide is formed as above. The quantum well-pump laser is shown with a U-shaped cavity with cleaved end-facet mirrors, although other diode laser structures could be used for either evanescent pumping or longitudinal pumping (via a waveguide Y-junction).

2. METAL-ION SPIN-ON GLASS WAVEGUIDES

We have selected polysiloxane spin-on glasses (SOGs) for the host matrix for the rare-earth ions. These materials are composed of polysiloxanes of compositions similar to $\{\text{SiO}_a(\text{CH}_3)_b(\text{OC}_2\text{H}_5)_c(\text{OH})_d\}$, $n=5-100$. These polymers are typically dissolved in mixed alcohol/ketone solvent systems for spin casting. After spin casting, a bake in a non-oxidizing atmosphere at temperature >400 °C drives condensation reactions that lead to loss of water and alcohols and the formation of a glass composed of Si, O and 4 to 11 wt. % C. These materials possess several characteristics that make them desirable hosts for wafer-level integration. One very important characteristic is the ability to form optical quality glass at temperatures sufficiently low to prevent III-V substrate or epi-layer degradation. These materials undergo condensation reactions leading to glassification at temperatures typically between 400 and 430 °C, which is compatible with a wide range of III-V materials. It is the requirement of such low temperatures that preclude the use of many previously developed techniques for incorporation of rare-earth ions into other higher-temperature glass matrices.

The undoped SOG materials possess a lower index of refraction than the doped MISOGs, which facilitates formation of the cladding layer of the waveguide. For example, typical polysiloxane SOGs have refractive indices at 633 nm of 1.38 ± 0.01 . Addition of the more polarizable rare-earths increases the refractive index in a linear fashion with concentration, as is illustrated in Fig. 2 for two different Accuglass formulations (Allied Signal).

Additional desirable properties include the moderate volume shrinkage during cure ($\approx 6\%$) and, the ability to spin-cast uniform, planar films ($<2\%$ thickness variation across a 6-inch wafer). Polysiloxane SOGs were developed for dielectric and planarization applications for silicon microelectronics. Consequently, they are available commercially in microelectronic grade purity and are etchable with F-based etchants, such as F-containing plasmas or HF-based wet etching solutions. Such etchants subject the III-V wafer to minimal attack during processing of the SOG material into optical device structures. Finally, the solvent systems used for various SOG formulations will readily dissolve rare earth salts such as the hydrated trichlorides or the acetylacetonates (2,4-pentanedionates).

We have employed three different SOG formulations in preparing the waveguides discussed here. The cladding layer (refractive index, $n = 1.37$ at 633 nm) is composed of a 1.5 to 1.7 μm layer of Hitachi HSG-2209 doped at 1 wt. % Nd^{3+} with $\text{NdCl}_3 \cdot 6\text{H}_2\text{O}$. This was applied by 5 or 6 spin-castings to achieve the desired thicknesses above with intermediate low temperature curing at temperatures less than 250 °C between spins to remove excess solvent. A 1-hour bake at $410 < T < 430$ °C condensed and glassified this composite cladding layer. Subsequently, the waveguiding layer was applied with either two spin-castings of 1 wt. % Nd^{3+} in an experimental Accuglass X615 (Allied Signal) ($n=1.44$) or with 8 spin-castings of 14 wt. % Nd^{3+} in Accuglass 111 (Allied Signal) ($n=1.43$). In Accuglass X615, Nd^{3+} was not required to increase the refractive index to permit formation of a waveguide. In contrast, the high concentration of Nd^{3+} in Accuglass 111 served to provide the requisite index difference for waveguiding.

The preceding structures were designed as waveguides for 1.06- μm light. Figure 3 shows the near-field pattern for 1.064- μm light for a slab waveguide made with 14 wt. % Nd^{3+} in Accuglass 111, the calculated fundamental mode profile in the direction perpendicular to the plane of the spin-on glass layers, and the measured fundamental mode profile in this same direction. Good confinement was obtained, and the measured transverse intensity profile is in good agreement with the calculated mode profile with no evidence of mode distortion due to the 8-spin castings used to form the waveguiding layer..

Prism refractometry measurements on the 1 wt. % Nd^{3+} doped Accuglass X615 samples were made at the 810-nm pump wavelength and give an effective refractive index consistent with the measured film refractive indices at 633 nm and the film thicknesses. Modal attenuation measurements could not be made with confidence on these samples since the free surface area was too restricted to use the sliding output prism technique. From the brightness and uniformity of the guided wave streak, however, we estimate the attenuation to fall roughly between 3 and 6 dB/cm at 810 nm and will be reduced at 1060 nm μm where the absorption is reduced.. Larger area samples will be fabricated in the near future so that modal attenuation measurements can be made at the pump (810 nm) and fluorescence (1050 nm) wavelengths. The 14 wt. % Nd^{3+} doped Accuglass 111 sample did not appear to waveguide at 810 nm, and subsequent spectral transmittance measurements indicate that the reduction in intensity due to Nd^{3+} absorption at 810 nm may be as high as 90 dB/cm. For the 1 wt. % Nd^{3+} doped sample, we imaged the guided-wave streak into an optical spectrum analyzer using a fast optical lens assembly and also

observed the m-line spectra using an output prism coupler. In this guided-wave test configuration, we did not observe fluorescence in the 1050-nm range when pumping at 514.5 nm or at 810 nm which we attribute in part to low input prism coupling efficiency. We estimate the input prism coupling efficiency is limited by waveguide surface topography to 10-20% at best. Reductions in particulate size and density and in edge bead removal will allow improved coupling efficiencies.

Fluorescence measurements in the 750-nm to 1250-nm wavelength range were carried out using a p-polarized CW 514.5-nm focused laser beam coupled into the waveguide layer at Brewster's angle (74.5°) for GaAs. This maximizes the available pump power and provides optical access for observing any fluorescence (and bandedge luminescence from the underlying GaAs) using fast collection optics aligned normal to the sample. This luminescence signal was fed to a fiber-coupled optical spectrum analyzer. As care was taken to avoid obvious scattering centers, the reflection from the sample surface was specular and very little pump power was coupled into the spectrometer. Figure 4 shows the measured fluorescence for the 1 wt. % Nd³⁺ doped Accuglass X615 sample and for an uncoated GaAs reference sample measured under the same conditions. These data were fitted over the range from 950 nm to 1150 nm using the sum of three terms (to minimize the number of free parameters): a Gaussian distribution to characterize the fluorescence at ca. 1050 nm, and the sum of a wavelength independent dc light level and a Gaussian distribution to simulate the effect of the tail of the GaAs bandedge luminescence in this range. The fluorescence spectrum is assumed to have a Gaussian distribution, consistent with inhomogeneous broadening, since the glass matrix has an amorphous structure. Our fitted results ($r^2=0.98$) for an incident pump power of 100 mW gives us a peak wavelength of about 1039 nm and a FWHM of 82 nm. At incident pump powers less than 5 mW, the peak wavelength is near 1050, as is typically observed in Nd-glass systems. The spectrometer resolution bandpass was set at 10 nm to increase our signal and was not deconvolved from these fitted results. Dependence of the fluorescence peak wavelength, FWHM, and intensity on input pump power and wavelength, rare-earth ion and doping density, and host matrix will be presented and discussed in a subsequent publication.

We inserted a commercial grade Nd:glass laser rod (Schott LG-660) into our test setup to assess the relative luminescence efficiency of our 1 wt. % Nd³⁺ doped Accuglass X615 sample. We find that the relative luminescence efficiency of our thin film sample appears to be between 12 and 57 times lower than that measured in the commercial bulk laser glass, depending on the volume correction factor used. We plan to conduct additional experiments to eliminate the uncertainty associated with estimating the volume correction factor for bulk vs. thin film samples and thereby provide a direct comparison of luminescence efficiency between our thin-film MISOG materials and commercial laser glass.

The relatively low quantum efficiency for emission in both Accuglass X615 and 111 can be understood in light of the probable interactions with the matrix. In the X615, the Nd³⁺ is introduced as the acetylacetonate (CH₃COCHCOCH₃⁻). Thus, both the SOG matrix and the counter anion are composed of relatively low mass elements (Si, O, C, and H). This can result in a matrix of relatively high phonon frequency, and consequently, a matrix that might promote quenching of the excited states of Nd through multiphonon relaxation (MPR) processes.^{3,4} In silicate glasses, MPR is facilitated by the RE-O-Si bond linkages, and one might expect such linkages to be important in this MISOG formulation.

If there is a low quantum efficiency in the Accuglass 111 MISOG material, it may have contributions from both multiphonon relaxation due to the relatively low-mass matrix and concentration quenching due to rare-earth-ion cluster formation.⁵ We have examined the Raman spectrum of 14% Nd³⁺ in Accuglass 111 to determine the probable types of Nd-matrix interaction (Fig 5). The major peaks can be assigned to either NdCl₃ or to Nd oxygen bonding, suggesting two or more types of sites are important in this matrix. The peaks at 150 and 208 cm⁻¹ correspond to the observed peaks at 150 and 210 in the Raman spectrum of NdF₃⁶, suggesting the inclusion of NdCl₃ microcrystallites in the SOG matrix at this high Nd concentration. The peaks at 119, 178, and 243 correspond to observed vibrations at 120, 180, and 242 in Y₂O₃ infrared spectra, which should be very similar to Nd₂O₃ due to similarities in mass and crystal structure.⁷ Since the symmetries of the Nd sites in the SOG matrix are not known, it is not clear whether strict adherence to crystal-based selection rules will occur in the glass matrix; so observation of features in the Raman spectrum at IR-allowed energies may be possible.

Additional evidence for microcrystallites in the very high concentration sample is provided by optical microscopy, where small crystallites ranging in size from 0.7 to 1.5 μm are observed. The existence of NdCl₃ microcrystals may be advantageous for increasing the luminescence quantum efficiency. The cross relaxation processes that result in concentration quenching can be alleviated by using an optically inactive rare-earth, such as La, to increase the refractive index, as required for waveguiding, but without optical quenching.⁸ The use of microcrystal formation for isolation of rare-earth ions from a high-phonon-

frequency matrix has been demonstrated by ion incorporation of ErF_3 and YbF_3 in PbCdF_x microcrystals to isolate rare-earths from the phonon bath of the silica glass matrix.⁹ A similar benefit may accrue from the microcrystals forming in SOG, if scattering is not a problem.

3. SUMMARY

Progress has been made in the development of rare-earth-doped spin-on glasses on III-V substrates as a new monolithic technology for developing compact infrared and visible (up-conversion) lasers, amplifiers, and other photonic integrated circuit components with semiconductor diode laser pumping. Slab waveguides have been demonstrated, and characterization of the optical properties of these materials suggests that, with further materials development, the goal of monolithic active waveguides and lasers can be achieved.

4. ACKNOWLEDGMENTS

The authors wish to acknowledge J.L. Dishman, C.T. Fuller, D.C. Meister, and M.S. Johnson for their technical assistance. This work was performed at Sandia National Laboratories and supported by the U.S. Department of Energy under Contract No. DE-AC04-94AL85000.

5. REFERENCES

1. E. Lallier, "Rare-Earth-Doped Glass and LiNbO_3 Waveguide Lasers and Optical Amplifiers," *Appl. Opt.* **31** (25), 5276 (1992).
2. M. Yanagisawa, H. Terui, K. Shuto, T. Miya, and M. Kobayashi, "Film-Level Hybrid Integration of AlGaAs Laser Diode with Glass Waveguide on Si Substrate," *IEEE Photon. Technol. Lett.* **4** (1), 21 (1992).
3. P. Urquhart, "Review of rare earth doped fibre lasers and amplifiers," *IEE Proceedings*, **135**, Pt. J (6), 385 (1988).
4. W. Lenth and R.M. Macfarlane, "Upconversion Lasers," *Opt. Photon. News* **3** (3), 8 (1992).
5. E. Desurvire, J.L. Zyskind, and C.R. Giles, "Design Optimization for Efficient Erbium-doped Fibre Amplifiers." *IEEE J. Lightwave Technol.* **8** (11) 1730 (1990).
6. R.P. Bauman and S.P.S. Porto, "Lattice Vibrations and Structure of Rare-Earth Fluorides," *Phys. Rev.* **161** (3), 842 (1967).
7. N.T. McDevitt and A.D. Davidson, "Infrared Lattice Spectra of Cubic Rare Earth Oxides in the Region 700 to 50 cm^{-1} ," *J. Opt. Soc. Am.*, **56** (5) 636 (1966).
8. M. Nakazawa and Y. Kimura "Lanthanum co-doped erbium fibre amplifier," *Electron. Lett.* **27** (12) 1065 (1991).
9. Y. Wang and J. Ohwaki, "New transparent vitroceraamics codoped with Er^{3+} and Yb^{3+} for efficient frequency upconversion," *Appl. Phys. Lett.* **63** (24), 3268 (1993).

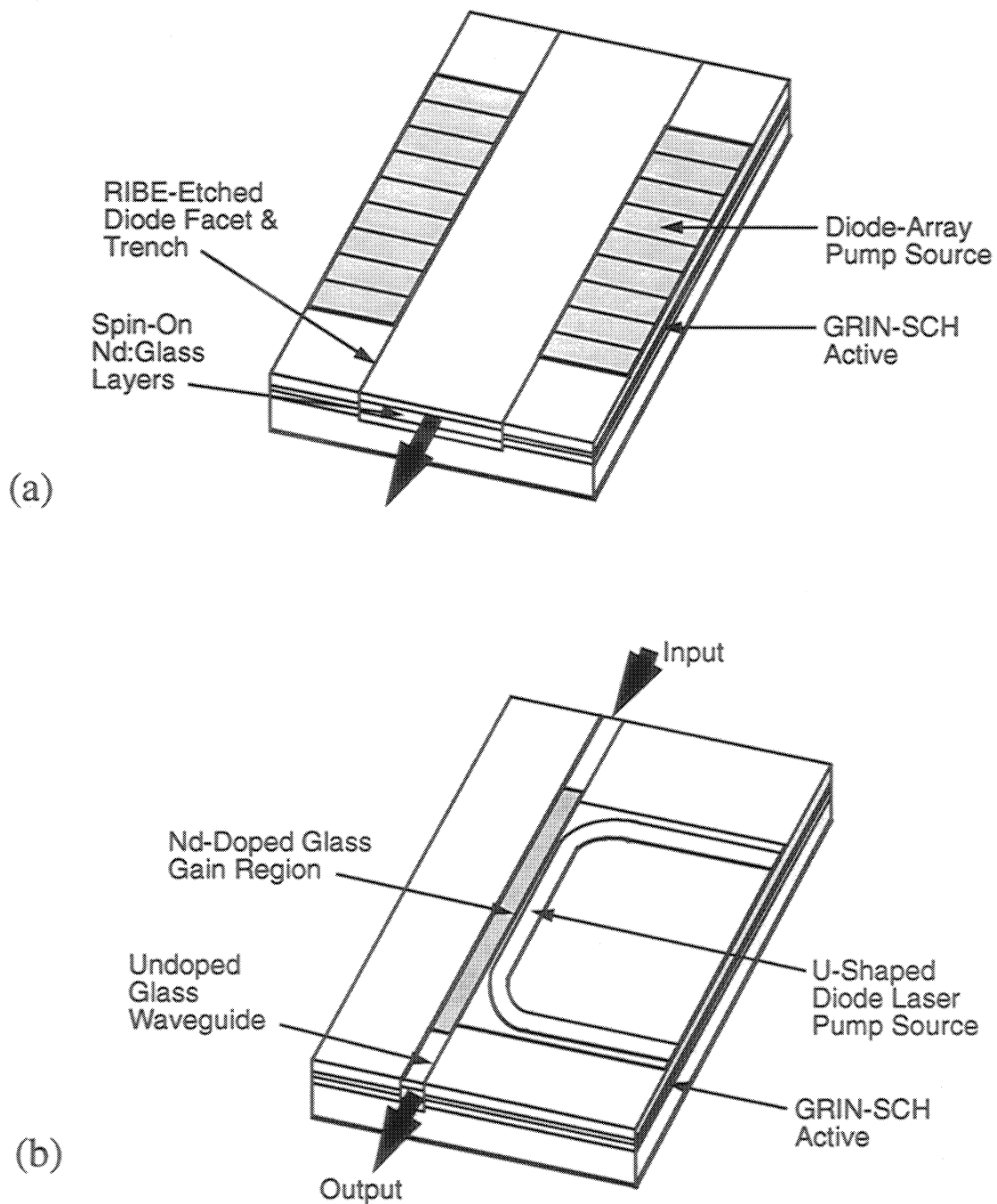


Figure 1. (a) High-power diode-array pumped Nd-doped spin-on glass laser or amplifier.
 (b) Evanescently pumped Nd-doped spin-on glass single-mode waveguide amplifier.

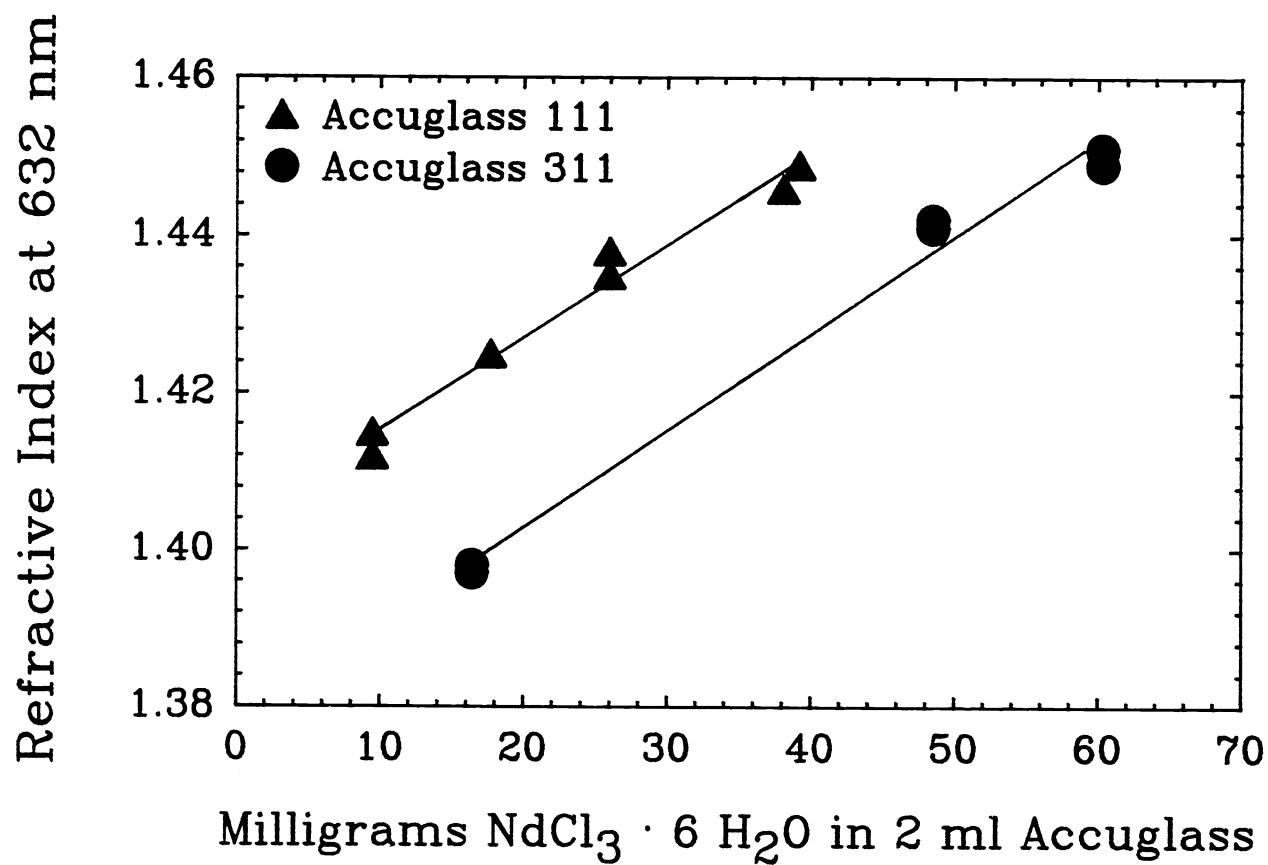
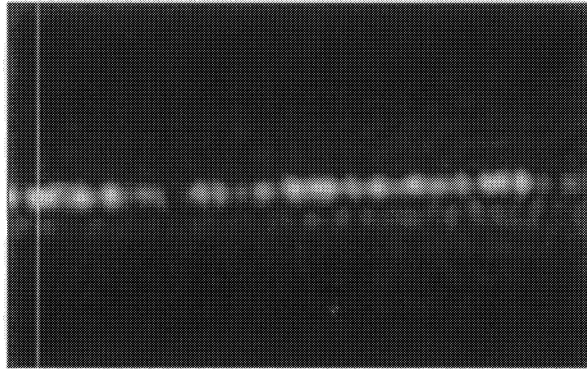
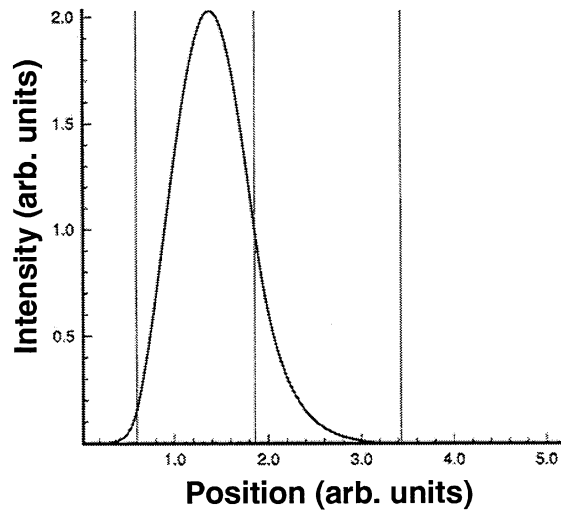


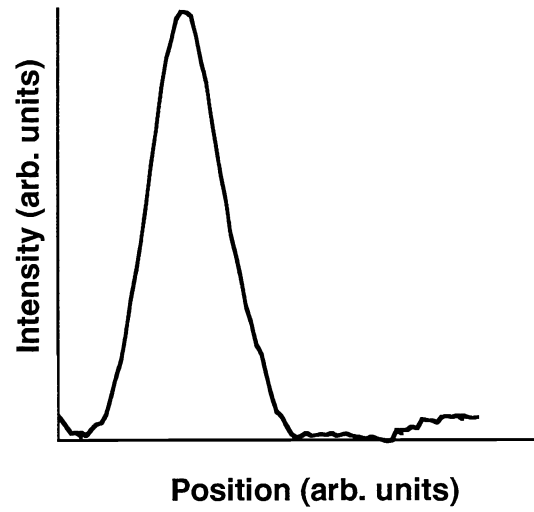
Fig. 2. Refractive index dependence on rare-earth-ion concentration.



(a)



(b)



(c)

Fig. 3: Waveguide in Nd:spin-on glass. Cladding layer: $1.57 \mu\text{m}$ 1 wt. % Nd^{3+} in HSG 2209, $n=1.37$. Guiding layer: 14 wt. % Nd^{3+} in Accuglass 111, $n=1.43$. Substrate: GaAs. a) Near-field image using $1.06\text{-}\mu\text{m}$ light. b) Calculated fundamental mode intensity profile of vertical cross-section perpendicular to plane of spin-on glass layers. c) Measured modal intensity profile.

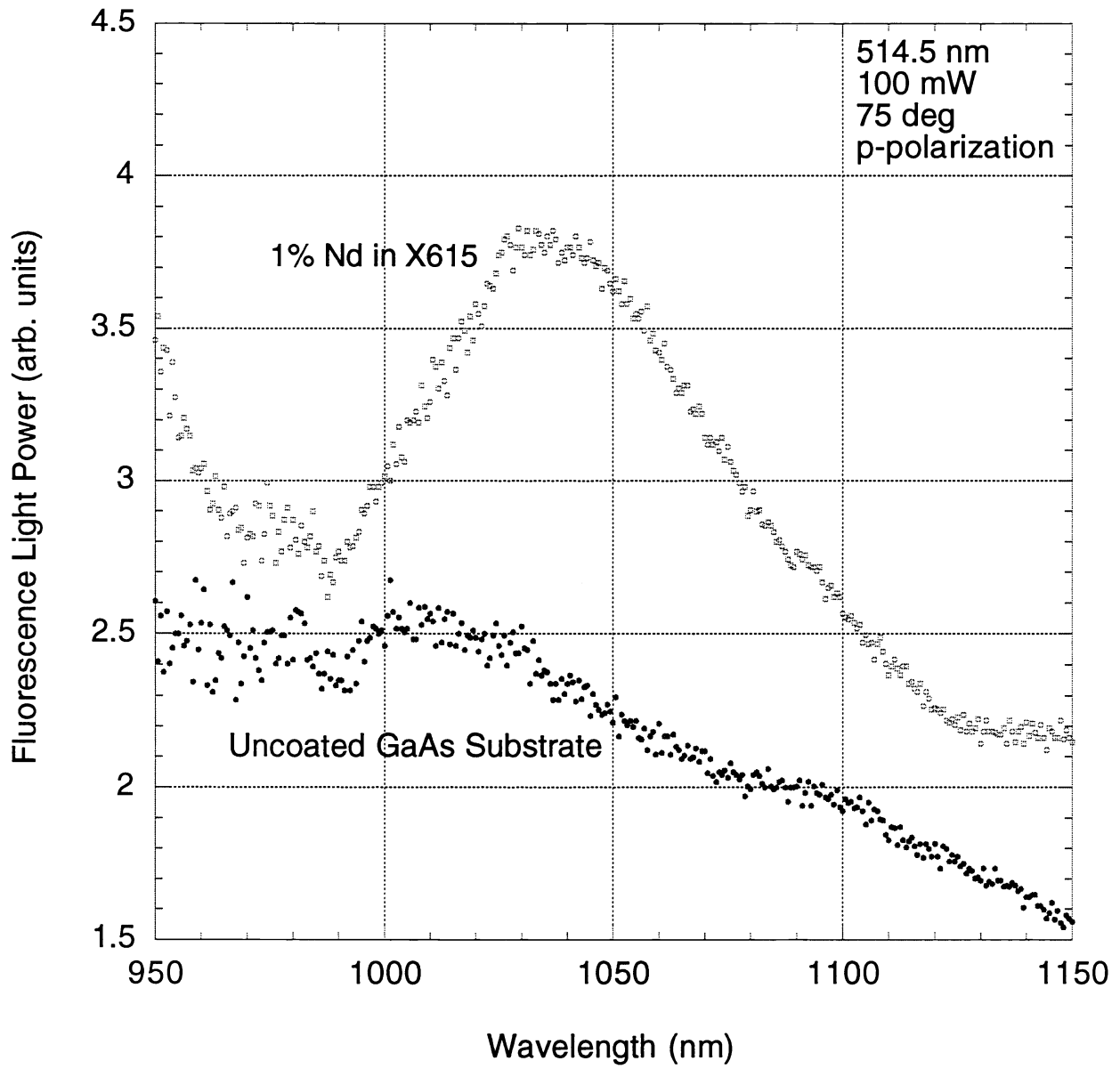


Fig. 4: Measured fluorescence spectra for 1% Nd in Accuglass X615 on GaAs and for an uncoated GaAs reference sample.

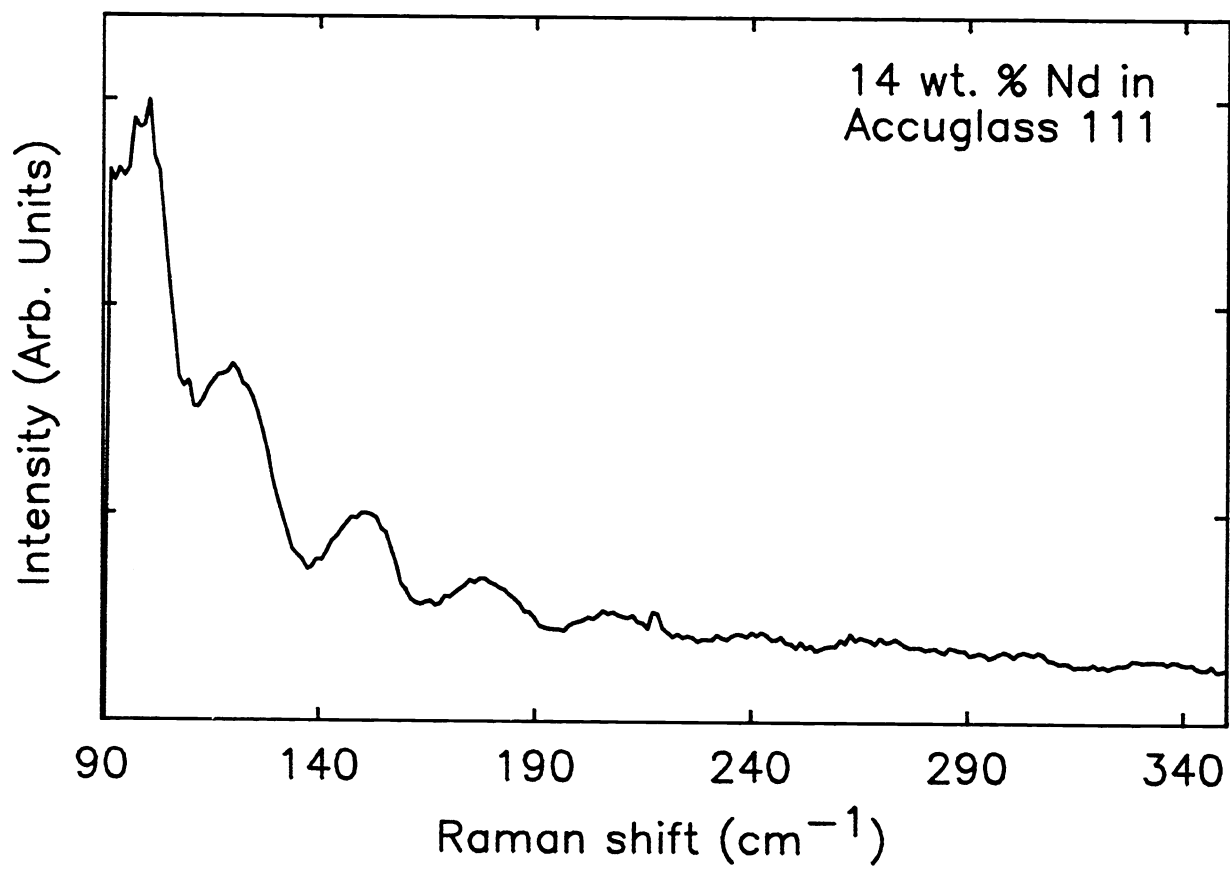


Fig. 5: Raman spectrum of 14 wt. % Nd^{3+} in Accuglass 111.(514.5-nm excitation)